Appl Phys B (2009) 95: 467–473
DOI 10.1007/s00340-009-3498-8

Applied Physics B
Lasers and Optics

Dispersion of electro-optic coefficients in sillenite crystals

A.T. Efremidis · N.C. Deliolanis · C. Manolikas · E.D. Vanidhis

Received: 5 December 2008 / Revised version: 15 February 2009 / Published online: 3 April 2009

Abstract The photorefractive crystals of the sillenite family ($Bi_{12}SiO_{20}$ or BSO, $Bi_{12}GeO_{20}$ or BGO, and $Bi_{12}TiO_{20}$ or BTO) that belong to the cubic 23 point group are optically active, and exhibit the piezoelectric, elasto-optic, electro-optic and electrogyration effect. In this paper we measure the dispersion of the electro-optic coefficient for all the crystals of the sillenite family in the visible spectral range (500–800 nm). For this we measure by ellipsometry the polarization properties of a beam transmitted in the transverse configuration under the action of an externally applied field. The experimental data are fitted with an analytical expression of the beam polarization to find the electro-optic coefficient. The results show a normal dispersion of the electro-optic coefficient in all three sillenite crystals, similarly to other electro-optic crystals.

PACS 42.70.Nq · 78.20.Jq · 42.65.Hw

1 Introduction

The crystals of the sillenite family exhibit the photorefractive effect and have been extensively studied and used in various applications, such as optical signal and image processing and dynamic holography and interferometry (see [1–6] and references herein). The sillenite family consists of three cubic crystals ($Bi_{12}SiO_{20}$, $Bi_{12}GeO_{20}$, and $Bi_{12}TiO_{20}$) that have 23 point group symmetry. Sillenites are photoconductive, and they exhibit optical activity, and the electro-optic, piezoelectric, elasto-optic, and electrogyration effects. The electro-optic effect is defined as the change of dielectric impermeability of a material (and consequently of its refractive index) under the influence of an electric field. The linear electro-optic effect (or Pockels effect) is exhibited in non-centrosymmetric crystals and is described by a third rank tensor [7, 8] and in the case of the 23 point group crystals there is only one independent electro-optic coefficient. Apart from the primary electro-optic effect there is a secondary mechanism: the electric field induces strain in the crystal (inverse piezoelectric effect), and the strain induces change in the refractive index (elasto-optic effect). When the electric field is homogeneous, the symmetry of the secondary electro-optic effect is the same as the primary [7], but for spatially modulated fields, such as in photorefractive gratings, the contribution of the secondary effect depends also on the grating orientation [9, 10].

There are various works on the electro-optic effect in the sillenite crystals; Lenzo et al. [11] and Aldrich et al. [12] were first to report values for BGO and BTO, but either without presenting the method or having an ambiguous analysis. In subsequent studies, the light propagation was correctly modeled by taking into account the optical activity, and the electro-optic coefficient was calculated using various crystal configurations and wavelengths, either by measuring the polarization characteristics of the beam exiting the crystal or finding the eigenstates of polarization [13–25]. There is a rather large deviation in the reported values: 3.5–5 pm/V for BSO and BGO, and they are a bit higher for BTO, and

A.T. Efremidis · N.C. Deliolanis (✉) · C. Manolikas · E.D. Vanidhis
Aristotle University of Thessaloniki, Department of Physics—Solid State Section, Thessaloniki 54630, Greece
e-mail: ndeli@physics.auth.gr
Fax: +30-2310-998019

Present address:
N.C. Deliolanis
Institute for Biological and Medical Imaging, Helmholtz Zentrum München, Ingolstädter Landstraße 1, Neuherberg 85764, Germany

they usually refer to different wavelengths and are measured by different methods. A major concern on the measurement of the electro-optic coefficient is the accurate evaluation of internal electric field. Apart from the externally applied field, space charge can be excited by the illuminating beams and build up inside the crystal, and consequently, change the spatial profile, and reduce the intensity of the external field. Proposed solutions to this problem are the use of low power beam to illuminate the crystal [15], the use of an extra UV beam to deplete the carriers [17], the calculation of the internal field through additional four wave mixing experiments [18], and corrections assuming phase integration [19], or the use of high frequency ac fields [22]. Another issue is about which electro-optic coefficient is actually measured; when the crystal is unclamped (free to deform) and the applied electric field is dc (or ac at a frequency lower than the acoustic resonance of the crystal [22], then the effective electro-optic coefficient is the combination of the primary and the secondary effect as described above, which is the most common case. Finally, despite the existence of some papers that report on measurements at different wavelengths [14, 15, 17, 22–25] there is not a clear picture on the variation of the electro-optic coefficient of the sillenites vs. wavelength. The reason is the use of either distinct laser lines, or bandpass filters.

In this paper we measure the electro-optic coefficient of all sillenite family crystals at the visible spectrum range. We use a grating monochromator to seamlessly scan the wavelength range, and we ellipsometrically record the polarization state of the output beam that is fitted to determine the unknown electro-optic coefficient. First, we present a thorough analysis of the propagation of light in sillenites using the Jones calculus, then we present the experimental and data processing details, and finally we discuss the results and the dispersion of the electro-optic and the similarities among similar crystal families.

2 Wave propagation in sillenites

The optical properties of a dielectric material can be deduced from the constitutive dielectric equation of the medium

$$\mathbf{D} = \varepsilon \mathbf{E}, \tag{1}$$

where ε is the dielectric permittivity that correlates the dielectric displacement $\mathbf{D}$ with the electric field $\mathbf{E}$. In the general case, the permittivity ε for dielectric anisotropic substances (crystals) is a hermitian second order tensor; its real symmetric component describes the birefringence and the antisymmetric imaginary component describes the optical activity (gyration). Equation (1) can thus be written as

$$\mathbf{D} = \mathrm{Re}(\varepsilon)\mathbf{E} + i\varepsilon_0 \mathbf{G} \times \mathbf{E} = \mathrm{Re}(\varepsilon)\mathbf{E} + i\varepsilon_0 G\mathbf{E}, \tag{2}$$

where $\mathbf{G}$ is the gyration vector. The vector product $\mathbf{G} \times \mathbf{E}$ can also be written as the matrix product $G\mathbf{E}$, where the elements of G are the projections of the gyration vector $\mathbf{G}$ to the principal axes:

$$G = \begin{pmatrix} 0 & -G_3 & G_2 \\ G_3 & 0 & -G_1 \\ -G_2 & G_1 & 0 \end{pmatrix} \tag{3}$$

and the magnitude of the gyration vector is $|G| = g_{ij} l_i l_j$, where g_{ij} is the gyration tensor and l_i and $l_j, i, j = 1, 2, 3$, are the projections of the normalized wave vector $\mathbf{k}/|k|$ to the principal crystallographic axes. Equivalently, the constitutive equation (2) can also be written as

$$\mathbf{E} = \frac{1}{\varepsilon_0} B\mathbf{D}, \tag{4}$$

where B is the impermeability second rank tensor. In the case of sillenites, where $\varepsilon_0 G \ll \varepsilon$, B can be expressed in terms of the real part B_R that describes birefringence only [26, 27]

$$B \simeq B_R - i B_R G B_R. \tag{5}$$

In the general case, the real part of the impermeability tensor B and the gyration tensor g have three independent coefficients, and for the crystals of the cubic system they are reduced to one.

The application of the electric field perturbs linearly both the elements of the real part of the impermeability tensor (Pockels electro-optic effect) and the gyration tensor (electrogyration). It should be mentioned that apart from the primary electro-optic effect there is a secondary contribution, which is the combination of the inverse piezoelectric and the elasto-optic; in the case of the 23 point group and for homogeneous electric field both the primary and the secondary effect have the same symmetry and the tensor coefficients are combined in a single effective electro-optic coefficient. The perturbations in the reduced form are [7, 8, 27]:

$$\Delta B_i = r_{ik} E_k \quad \text{and} \quad \Delta g_i = \zeta_{ik} E_k, \tag{6}$$

where $i = 1, 2, \ldots, 6$, $k = 1, 2, 3$, E_k are the components of the electric field, r_{ik} and z_{ik} are the 6×3 reduced tensor forms of the effective electro-optic and the electrogyration coefficient and the index i corresponds to the elements of the B and G tensors according to the following transformations $11 \to 1$, $22 \to 2$, $33 \to 3$ $23 = 32 \to 4$, $13 = 31 \to 5$, $12 = 21 \to 6$. The elements for all the above mentioned tensors at the cubic system are presented in Table 1 expressed in the crystallographic coordinates $\{x_1, x_2, x_3\}$ and using the abbreviated notation [7].

Light propagation in crystals can be generally modeled into two orthogonally-polarized elliptical field components

Table 1 The tensors of the optical properties of the sillenite crystals (class 23) expressed in the crystallographic coordinates

Impermeability	Gyration	Electro-optic	Electrogyration
$\begin{pmatrix} 1/n^2 & 0 & 0 \\ 0 & 1/n^2 & 0 \\ 0 & 0 & 1/n^2 \end{pmatrix}$	$\begin{pmatrix} g_{11} & 0 & 0 \\ 0 & g_{11} & 0 \\ 0 & 0 & g_{11} \end{pmatrix}$	$\begin{pmatrix} 0 & 0 & 0 \\ 0 & 0 & 0 \\ 0 & 0 & 0 \\ r_{41} & 0 & 0 \\ 0 & r_{41} & 0 \\ 0 & 0 & r_{41} \end{pmatrix}$	$\begin{pmatrix} 0 & 0 & 0 \\ 0 & 0 & 0 \\ 0 & 0 & 0 \\ \zeta_{41} & 0 & 0 \\ 0 & \zeta_{41} & 0 \\ 0 & 0 & \zeta_{41} \end{pmatrix}$

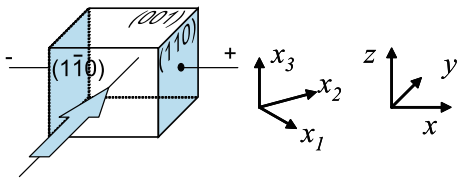

Fig. 1 The crystal configuration, the crystallographic and the external coordinate system. Light propagates along the y-axis, while the electric field is applied along the x-axis

that have opposite sense of rotation and that propagate with two different phase velocities along the wave normal $\mathbf{k}/|k|$. Herein is a brief step-by-step analysis: the impermeability tensor B, which is expressed in the crystallographic coordinate system, is rotated to a new orthogonal coordinate system that has one axis parallel to the wave normal direction $\mathbf{k}/|k|$. The new transformed tensor B' is given by the transformation equation $B' = aBa^T$, where α and α^T are the 3×3 (unitary) transformation matrix between the coordinate systems and its transpose. The polarization state of components and their corresponding velocities are the solutions of the eigenvalue problem of a transformed impermeability tensor B' [26]

$$B'\mathbf{D}_i = \frac{1}{n_i^2}\mathbf{D}_i, \tag{7}$$

where, $\mathbf{D}_i$ are the eigenpolarizations, n_i are the corresponding refractive indices, and $i = 1, 2, 3$. The two orthogonal components are those two (out of three) solutions of (7) that are perpendicular to the wave normal $\mathbf{k}/|k|$. Or equivalently, the polarization components are described by the two eigenvalue problem solutions of a reduced 2×2 matrix B'', which is derived from B' by striking out the line and column that correspond to the direction of propagation.

For the measurement of the electro-optic coefficient we have chosen the "transverse configuration", where the crystal front face is the (1$\bar{1}$0) and the electric field is applied along the [110] direction (Fig. 1). The "transverse configuration" is the most common configuration for two-mixing applications and additionally the contribution of the electrogyration coefficient is cancelled. For this configuration the tensor transformed to the external coordinate system and reduced to 2×2 is

$$B'' = \begin{bmatrix} 1/n^2 & rE_0 - i\,g/n^4 \\ rE_0 + i\,g/n^4 & 1/n^2 \end{bmatrix}, \tag{8}$$

where E_0 is the strength of the applied electric field.

With the help of the table B'' the eigenvalues $1/n_{1,2}^2$ and the eigenstates $\mathbf{D}_{1,2}$ for transmission to direction [1$\bar{1}$0] were calculated to be:

$$\mathbf{D}_1 = \frac{1}{\sqrt{2}}\begin{pmatrix} 1 \\ -e^{-iA} \end{pmatrix}, \qquad \mathbf{D}_2 = \frac{1}{\sqrt{2}}\begin{pmatrix} e^{iA} \\ 1 \end{pmatrix}, \tag{9a}$$

where

$$A = -\arctan\frac{g}{rE_0 n^4} \tag{9b}$$

and

$$\frac{1}{n_{1,2}^2} = \frac{1}{n^2}\left(1 \mp \sqrt{n^4 r^2 E_0^2 + \frac{g^2}{n^4}}\right). \tag{10}$$

Finally, the light intensity I after transmission length l into the crystal and emerging from an analyzer has the form

$$I = \frac{1}{2}\{1 + \cos 2\theta\left[\cos^2 A + \cos(\phi_1 - \phi_2)\sin^2 A\right] + \sin A \sin 2\theta \sin(\phi_1 - \phi_2)\}, \tag{11}$$

where θ is the analyzer angle in from the [110] direction and $\phi_{1,2} = \frac{2\pi}{\lambda}n_{1,2}$ is the phase retardation for the two eigenstates.

3 Experiment and data processing

The experimental setup consists of the illumination system, a base to hold, translate, tilt, and rotate the crystal for accurate placement, and the detection system. In the illumination system the light from a current stabilized incandescent lamp is collected in a reflecting-grating monochromator with an exit slit 0.5 mm wide that provides a bandwidth of 2 nm. The light is collected with a double achromatic condenser system and then collimated to illuminate the front face of the

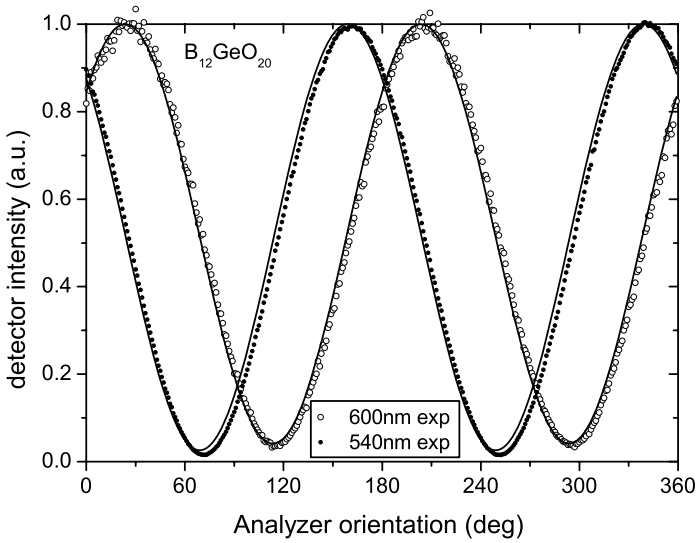

Fig. 2 Experimentally measured intensity (*dotted line*) of BGO at 540 nm (*black dots*) and 600 nm (*white circles*) acquired when $E_0 = 7$ kV/cm is externally applied as a function of the analyzer orientation angle θ from [110]. The data are fitted with the theoretical formula for the electro-optic coefficient (*solid lines*)

crystal. The crystals used in the experiment were provided from Fujian Chastech (P.R. China) and were rectangular parallelepipeds cut along the (110), $(1\bar{1}0)$, and (001) planes with an accuracy of 0.5° and polishing better than $\lambda/4$ at the $(1\bar{1}0)$ faces. The dimensions $x \times y \times z$ of the crystals were $9.1 \times 5.43 \times 10.01$ mm^3 for BSO, $9 \times 5.5 \times 10$ mm^3 for BGO, and $7.97 \times 7.92 \times 7.98$ mm^3 for BTO. A crystal polarizer is positioned in the beam path before the crystal with its polarization plane parallel to [110]. The crystal is placed between two large parallel cooper plates that are connected to a high-voltage power supply to create a homogeneous electric field. The intensity of the light incident on the crystal is less than 20 nW/cm^2 in order to avoid the excitation of electrons and minimize the build up of space charge due to the electron drift under the applied electric field. A Polaroid-film polarizer mounted on a 0.01°-step motorized rotating stage is placed after the crystal to analyze the polarization state of the transmitted beam. The light is focused in a 1 mm pinhole and the light intensity is detected with a photomultiplier tube and measured with a 6-digit multimeter.

In Fig. 2 the intensity vs. analyzer orientation is presented for a BGO crystal when 7 kV/cm are applied along [110]. Assuming that the optical properties of the crystal are known, the experimental data can be fitted with the theoretical intensity formula of (11). For this we have measured the optical activity of the same samples in the visible range 500–800 nm on the same setup, while the values of the refractive index are taken from [28]. Additionally, we measured the dispersion of the absorption coefficient for all three crystals, by subtracting the reflectance from the transmittance over the 500–800 nm range. The experimental intensity data were fitted with the Levenberg-Marquardt algorithm optimizing for the unknown electro-optic coefficient. For the data of Fig. 2, the electro-optic coefficient value is 4.1 and 3.8 pm/V at 540 and 600 nm respectively.

4 Results and discussion

In Figs. 3, 4, and 5, the calculated electro-optic coefficient for the three sillenite crystals are presented; The values are the mean of the 3 measurements recorded at 7 kV/cm, and they fall within those previously reported in the literature (see Table 2 for the comparative results): for BSO the r_{41} is 4.2–2.0 pm/V at the 500–800 nm range with an average error 0.1 pm/V, for BGO it is 4.4–2.4 pm/V, with an average error 0.2 pm/V, and 5.7–2.6 pm/V for BTO with an average error of 0.1 pm/V. The error is variable because the change of the transmitted beam ellipticity with the electric field is variable, and thus, when in some wavelengths this change is small, the error increases. The optical activity is ranging between 40–12 deg/mm for BSO, 42–12 deg/mm for BGO, and 12–3.6 deg/mm for BTO; these values also agree with previously reported results [28].

From previous photorefractive experiments in sillenite crystals [29] 0.4 mJ/cm^2 of exposure at the absorbing wavelength range (<560 nm) created an opposite static internal field that decreased the applied field up to 40–50%. In this experiment the exposure per measurement is 0.6 μJ/cm^2 (almost 3 orders of magnitude less) and we assume that this intensity is not enough to develop a screening field in the non-absorbing spectral range of the crystals (600–800 nm). To test this, we have measured the electro-optic coefficient at a non-absorbing wavelength (700 nm), before and after attempting to create a static internal field. The crystal was illuminated at 580 nm with the same exposure as the measurements reported before, but we did not observe any change in the polarization state (and the calculated electro-optic coefficient) at 700 nm. However, it may be possible that space charge field builds-up bellow 560 nm, which in turn can potentially influence (decrease) the calculated value of the electro-optic coefficient.

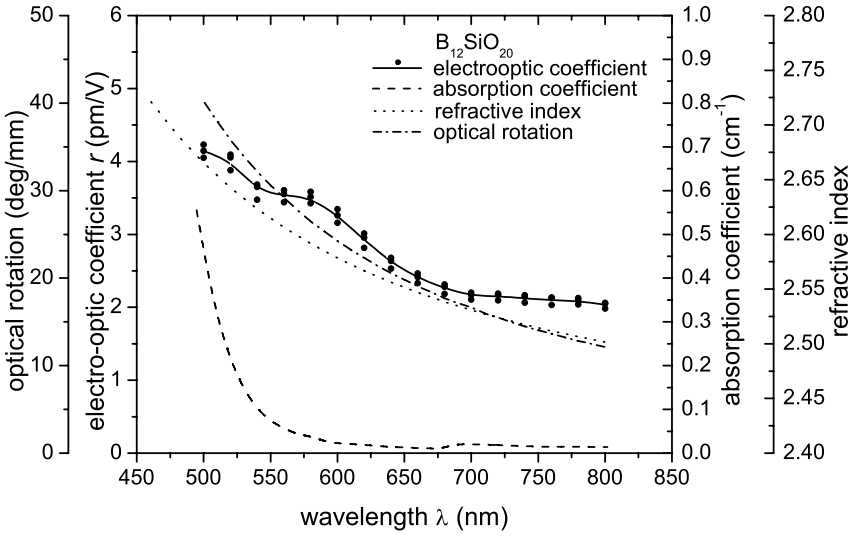

Fig. 3 Electro-optic coefficient, refractive index, optical activity, and absorption coefficient of BSO. *Dots* are for experimental data from 3 sets, *solid line* is for the average

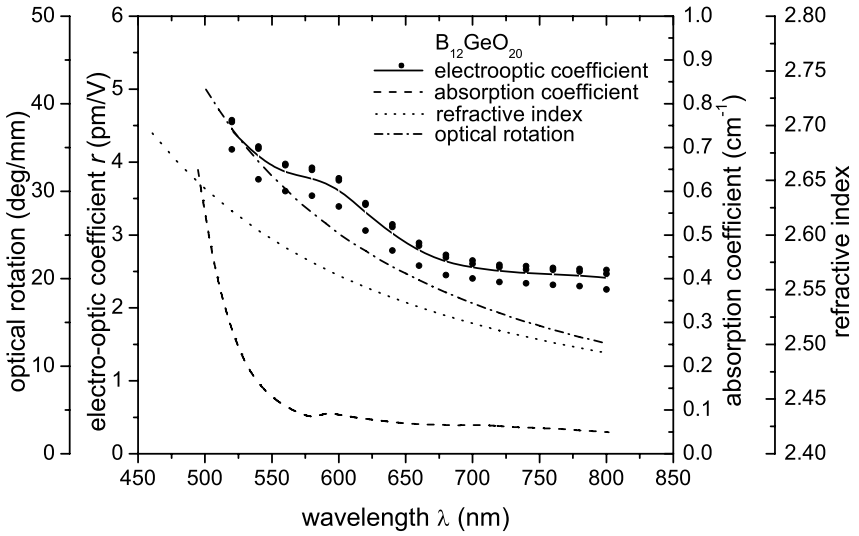

Fig. 4 Electro-optic coefficient, refractive index, optical activity, and absorption coefficient of BGO. *Dots* are for experimental data from 3 sets, *solid line* is for the average

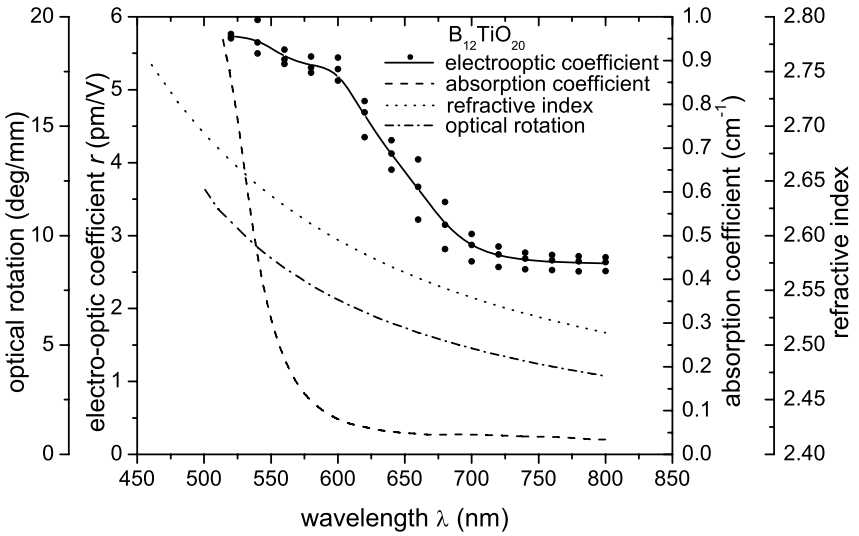

Fig. 5 Electro-optic coefficient, refractive index, optical activity, and absorption coefficient of BTO. *Dots* are for experimental data from 3 sets, *solid line* is for the average

Table 2 Comparative results for the electro-optic coefficient r_{41} for the sillenite crystal family. Units are pm/V for the r_{41} and nm for the wavelengths (in parentheses)

Publication	BSO	BGO	BTO	details
Fox et al. [13]			5.17 (633)	
Pellat-Finet et al. [14]	3.6 (450–700)			No dispersion
Henry et al. [15]	4.1 (633–700)			Mean value
Vachss et al. [16]	5.0 (633)	4.1 (633)		
Bayvel et al. [17]	4.2 (633), 3.8 (850)	3.7 (633), 3.3 (850)		Indication of dispersion
Wilde et al. [18]			5.8 (633)	
Lemaire et al. [19]	∼4.0 (650)			
Lemaire et al. [21]	∼3.8 (650)	∼3.3 (650)	∼2.1 (650)	
Grunnet-Jepsen et al. [22]	4.4 (633)			
Papazoglou et al. [23]			5.3 (550–660)	Mean value
Han et al. [24]	3.4–5.1 (488–633)			No dispersion (scattered measurements)
Kim et al. [25]	3.5–5 (488–633)			No dispersion reported
This paper	4.2–2 (520–800)	4.4–2.4 (520–800)	5.7–2.6 (520–800)	

Dispersion of the electro-optic coefficient has been recently studied in cerium-doped strontium barium niobate (SBN, point group symmetry $4mm$) [30], lithium tantalate ($LiTaO_3$) [31], in lead magnesium niobate lead titanate [32], undoped and magnesium doped lithium niobate ($LiNbO_3$) [33, 34]. The wavelength dependence is observed near the absorption edge and is described with the Sellmeier-type dispersion equations introduced by Di Domenico and Wemple [35] that relate the electro-optic effect with the polarization potentials in ferroelectrics. Electro-optic effect dispersion has not been detected in the sillenite family before, however from Figs. 3–5 it seems that such a dependence on wavelength exists. It is taking place near the absorption edge of the sillenite crystals, and is similar to the dispersion of the refractive index, the optical activity and the electrogyration effect [28].

In this paper we have presented the measurements of the electro-optic coefficient of the sillenite family by measuring the change in the optical properties with the applied electric field. The use of a grating monochromator has enabled the seamless acquisition of experimental data over a wide range in the visible spectrum (500–800 nm) and has revealed the dispersion of the electro-optic effect. The values of the electro-optic coefficient are in agreement with most of those previously reported in the literature.

References

1. P. Yeh, *Introduction to Photorefractive Nonlinear Optics*. Wiley Series in Pure and Applied Optics (Wiley, New York, 1993)
2. P. Günter, J.-P. Huignard (eds.), *Photorefractive Materials and Their Applications, 1*. Springer Series in Optical Sciences, vol. 113 (Springer, Berlin, 2006)
3. P. Günter, J.-P. Huignard (eds.), *Photorefractive Materials and Their Applications, 2*. Springer Series in Optical Sciences, vol. 114 (Springer, Berlin, 2007)
4. P. Günter, J.-P. Huignard (eds.), *Photorefractive Materials and Their Applications, 3*. Springer Series in Optical Sciences, vol. 115 (Springer, Berlin, 2007)
5. L. Solymar, D.J. Webb, A. Grunnet-Jepsen, *The Physics and Applications of Photorefractive Materials* (Clarendon, Oxford, 1996)
6. C. Gu, Y. Xu, Y.S. Liu, J.J. Pan, F.Q. Zhou, H. He, Opt. Mater. **23**, 219 (2003)
7. J.F. Nye, *Physical Properties of Crystals* (Oxford University Press, Oxford, 1957)
8. Y.I. Sirotin, M.P. Shaskolskaya, *Fundamentals of Crystal Physics* (Mir, Moscow, 1982)
9. S.I. Stepanov, S.M. Shandarov, N.D. Khatkov, Sov. Phys. Solid State. (Fiz. Tverd. Tela) **29**, 1754 (1987)
10. S.M. Shandarov, V.V. Shepelevich, N.D. Khatkov, Opt. Spektrosk. **70**, 1068 (1991)
11. P.V. Lenzo, E.G. Spencer, A.A. Ballman, Appl. Opt. **5**, 1688 (1966)
12. R.E. Aldrich, S.L. Hou, M.L. Harvill, J. Appl. Phys. **42**, 493 (1971)
13. A.J. Fox, T.M. Bruton, Appl. Phys. Lett. **27**, 360 (1975)
14. P. Pellatfinet, Opt. Commun. **50**, 275 (1984)
15. M. Henry, S. Mallick, D. Rouede, L.E. Celaya, A.G. Weidner, J. Appl. Phys. **59**, 2650 (1986)
16. F. Vachss, L. Hesselink, Opt. Commun. **62**, 159 (1987)
17. P. Bayvel, M. McCall, R.V. Wright, Opt. Lett. **13**, 27 (1988)
18. J.P. Wilde, L. Hesselink, S.W. McCahon, M.B. Klein, D. Rytz, B.A. Wechsler, J. Appl. Phys. **67**, 2245 (1990)
19. P. Lemaire, M. Georges, Opt. Lett. **17**, 1411 (1992)
20. P. Lemaire, M. Georges, Opt. Commun. **91**, 260 (1992)
21. P.C. Lemaire, M.P. Georges, Opt. Mater. **4**, 182 (1995)
22. A. Grunnet-Jepsen, I. Aubrecht, L. Solymar, J. Opt. Soc. Am. B, Opt. Phys. **12**, 921 (1995)
23. D.G. Papazoglou, A.G. Apostolidis, E.D. Vanidhis, Appl. Phys. B, Lasers Opt. **65**, 499 (1997)
24. S.H. Han, J.W. Wu, J. Opt. Soc. Am. B, Opt. Phys. **17**, 1205 (2000)

25. A. Kim, J.W. Wu, S.H. Han, B. Park, H. Takezoe, J. Nonlinear Opt. Phys. Mater. **13**, 397 (2004)
26. A. Yariv, P. Yeh, *Optical Waves in Crystals* (Wiley, New York, 1984)
27. T.A. Maldonado, T.K. Gaylord, Appl. Opt. **28**, 2075 (1989)
28. N.C. Deliolanis, E.D. Vanidhis, N.A. Vainos, Appl. Phys. B, Lasers Opt. **85**, 591 (2006)
29. N.C. Deliolanis, I.M. Kourmoulis, A.G. Apostolidis, E.D. Vanidhis, D.G. Papazoglou, Phys. Rev. E **68**, 17 (2003)
30. M. Imlau, K. Bastwoste, S. Moller, U. Voelker, M. Goulkov, J. Appl. Phys. **100**, 6 (2006)
31. H.L. Saadon, N. Theofanous, M. Aillerie, J. Phys. D, Appl. Phys. **39**, 2509 (2006)
32. C.J. He, W.W. Ge, X.Y. Zhao, H.Q. Xu, H.S. Luo, Z. Zhou, J. Appl. Phys. **100**, 4 (2006)
33. K. Yonekura, L. Jin, K. Takizawa, Opt. Rev. **14**, 194 (2007)
34. K. Yonekura, L.H. Jin, K. Takizawa, Jpn. J. Appl. Phys. **47**, 5503 (2008)
35. M. DiDomenico, S.H. Wemple, J. Appl. Phys. **40**, 720 (1969)